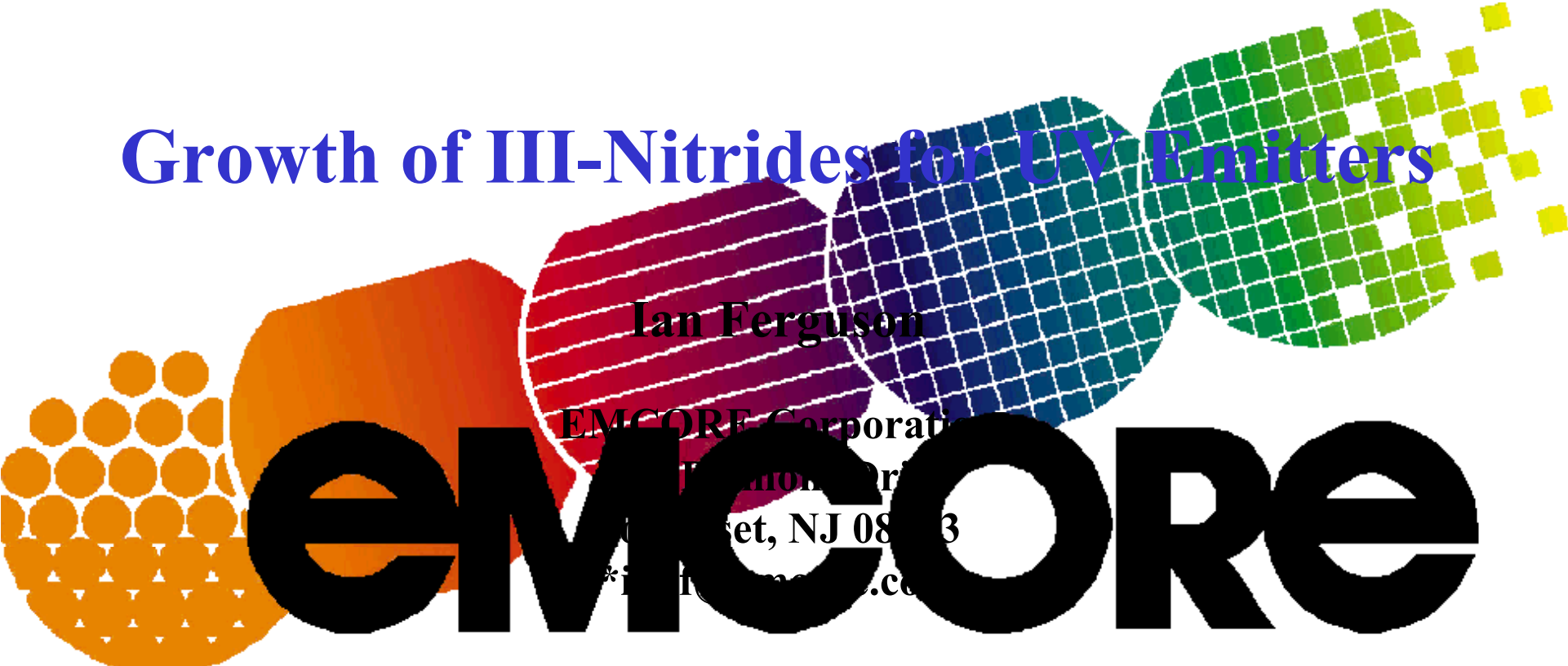




Growth of III-Nitrides for UV Emitters



Ian Ferguson

EMCORE Corporation

100 Morris Avenue

Bridgewater, NJ 08807

*info@emcore.com

Outline

- 
- **Introduction**
 - **Growth of GaN based materials**
 - **AlGaN materials growth**
 - **UV p-i-n photodetector devices results**
 - **Conclusions**

Technical Challenges and Issues



Materials development:

- High quality ($x=0.4-0.6$) $\text{Al}_x\text{Ga}_{1-x}\text{N}$
- p-doping, Mg incorporation
- Contacts to p-AlGaN
- Cladding layers
- Lower dislocation densities
- Eliminate cracking

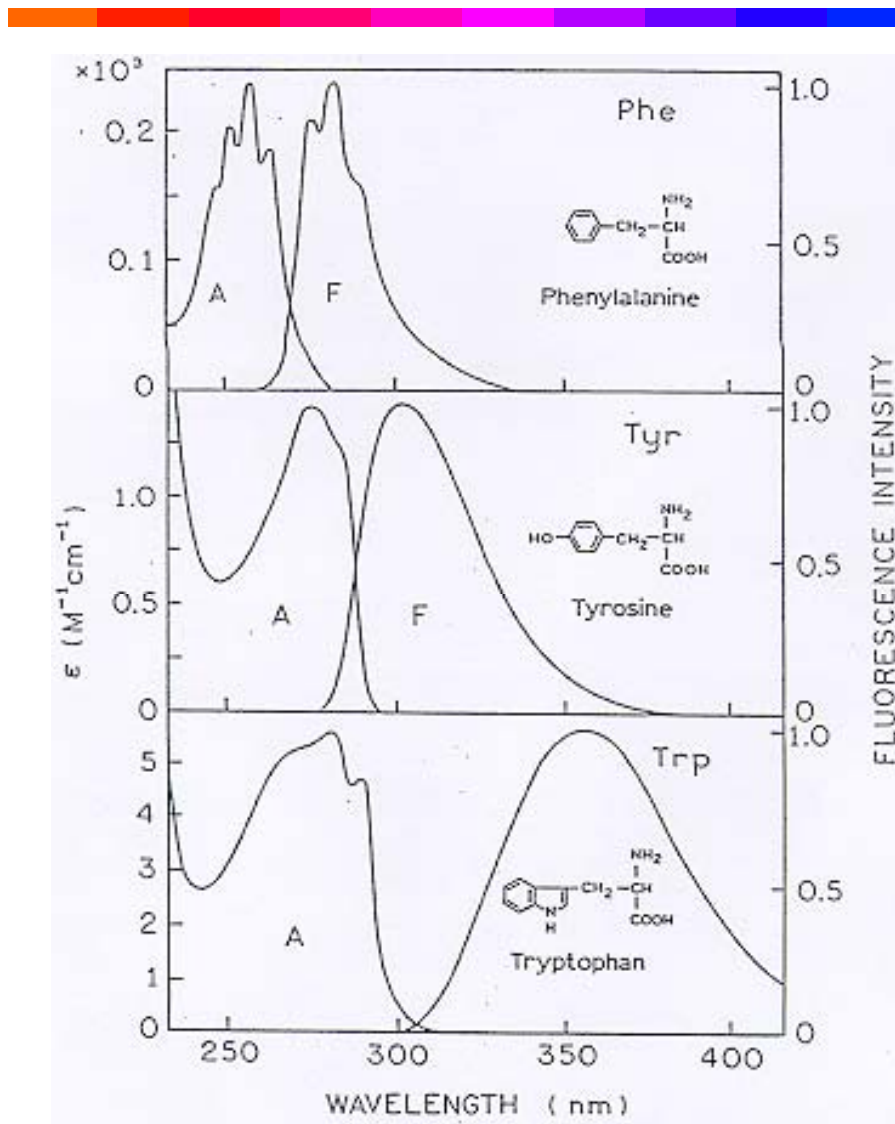
Growth on nearly lattice-matched UV transparent substrate materials:

- AlN or AlGaN substrates

Improved characterization techniques:

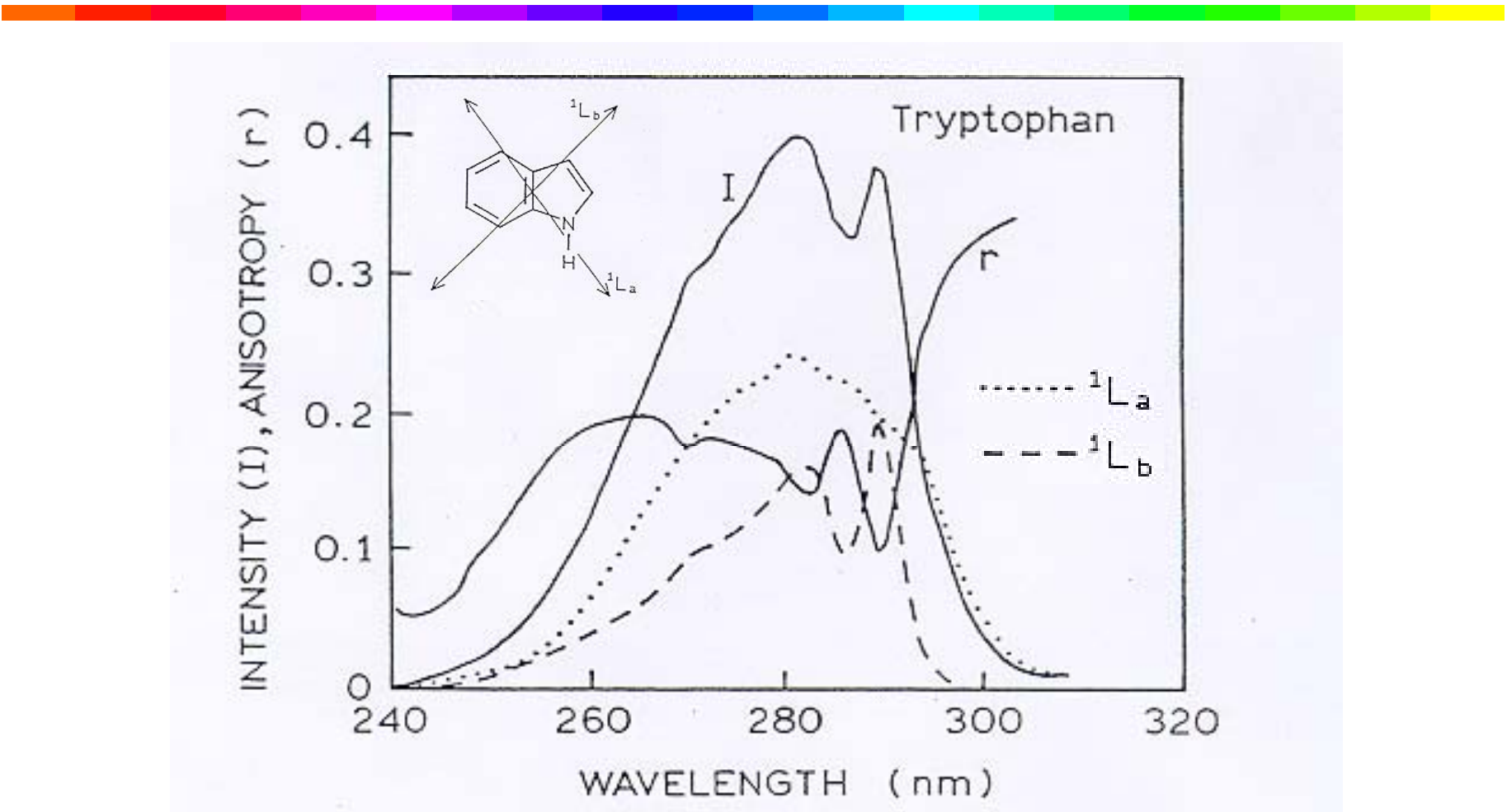
- PL, SIMS, UV transmission/absorption and Micro-Raman
- x-mapping techniques

Intrinsic protein fluorescence is due to aromatic amino acids



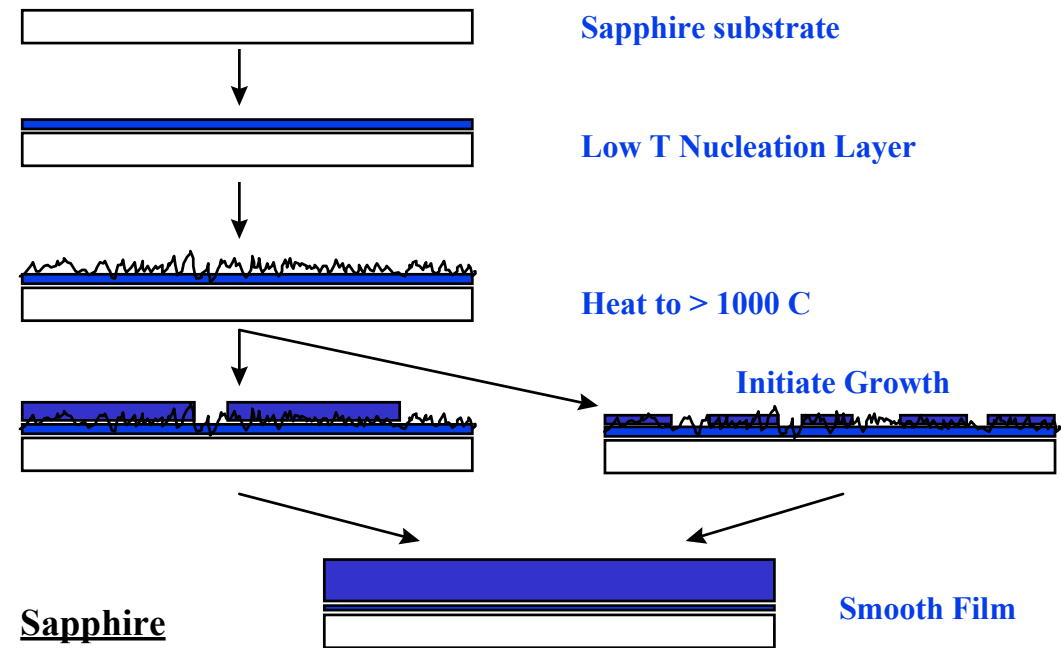
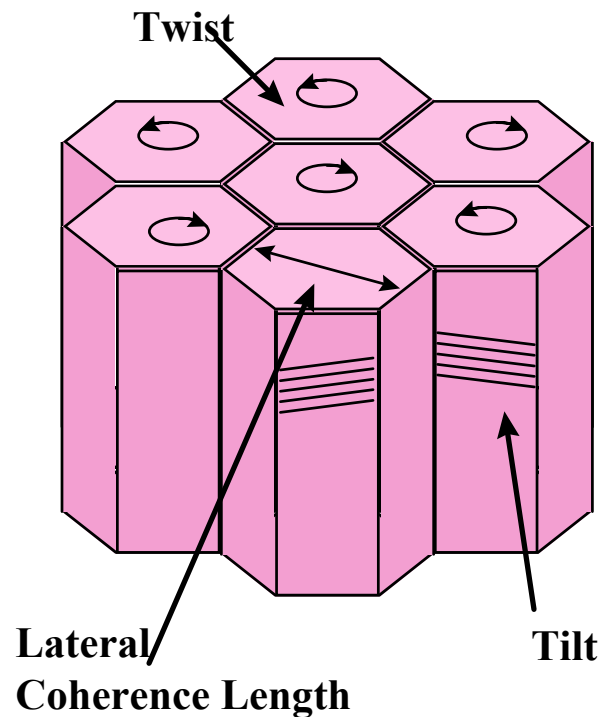
- Tryptophan dominates the intrinsic fluorescence of proteins
- Most proteins include Tyrosine and Tryptophan

Tryptophan has complex spectral properties



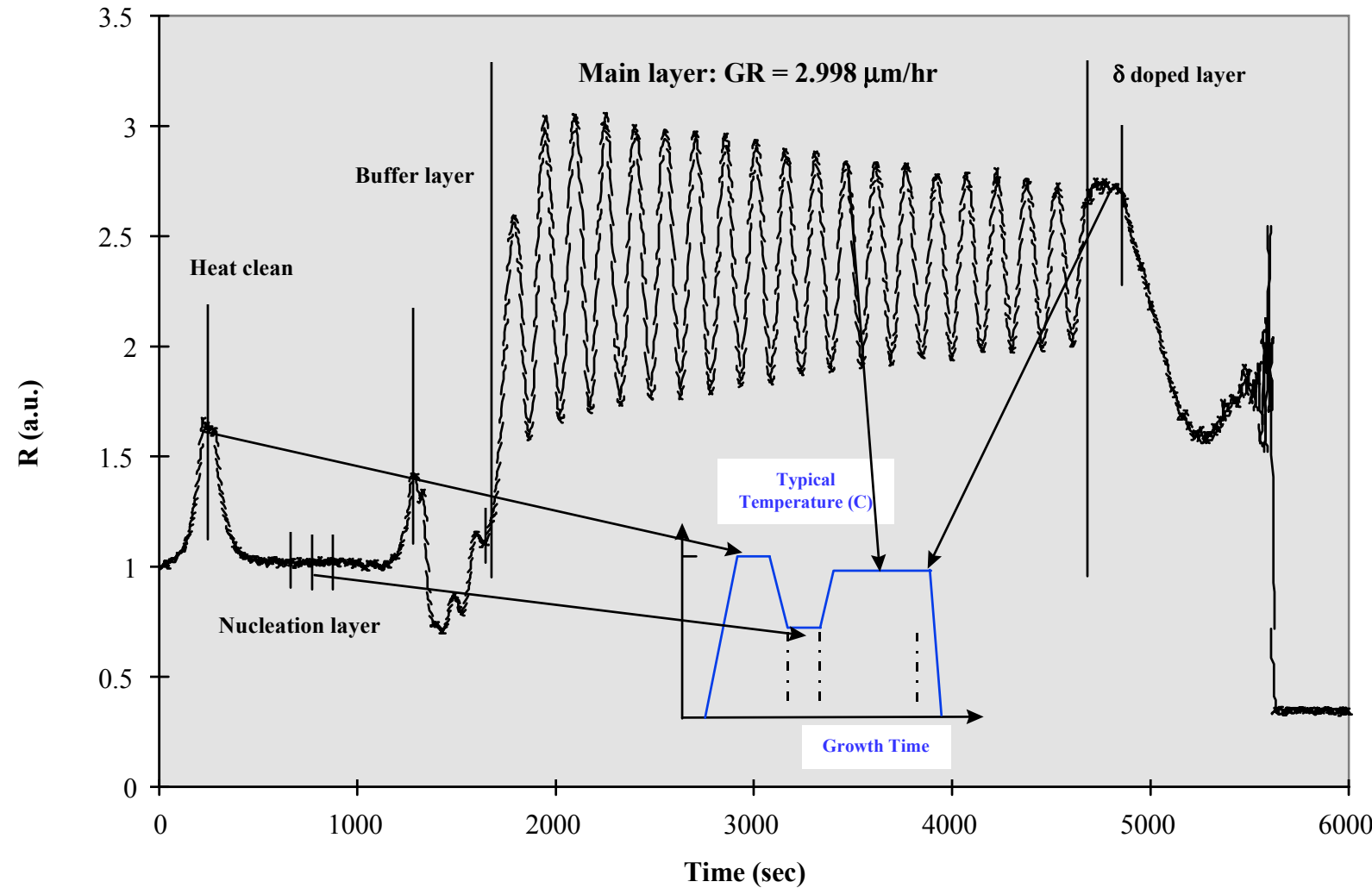
Excite at 295 nm because it does not excite tyrosine and the isotropy is simplified

GaN domain structure

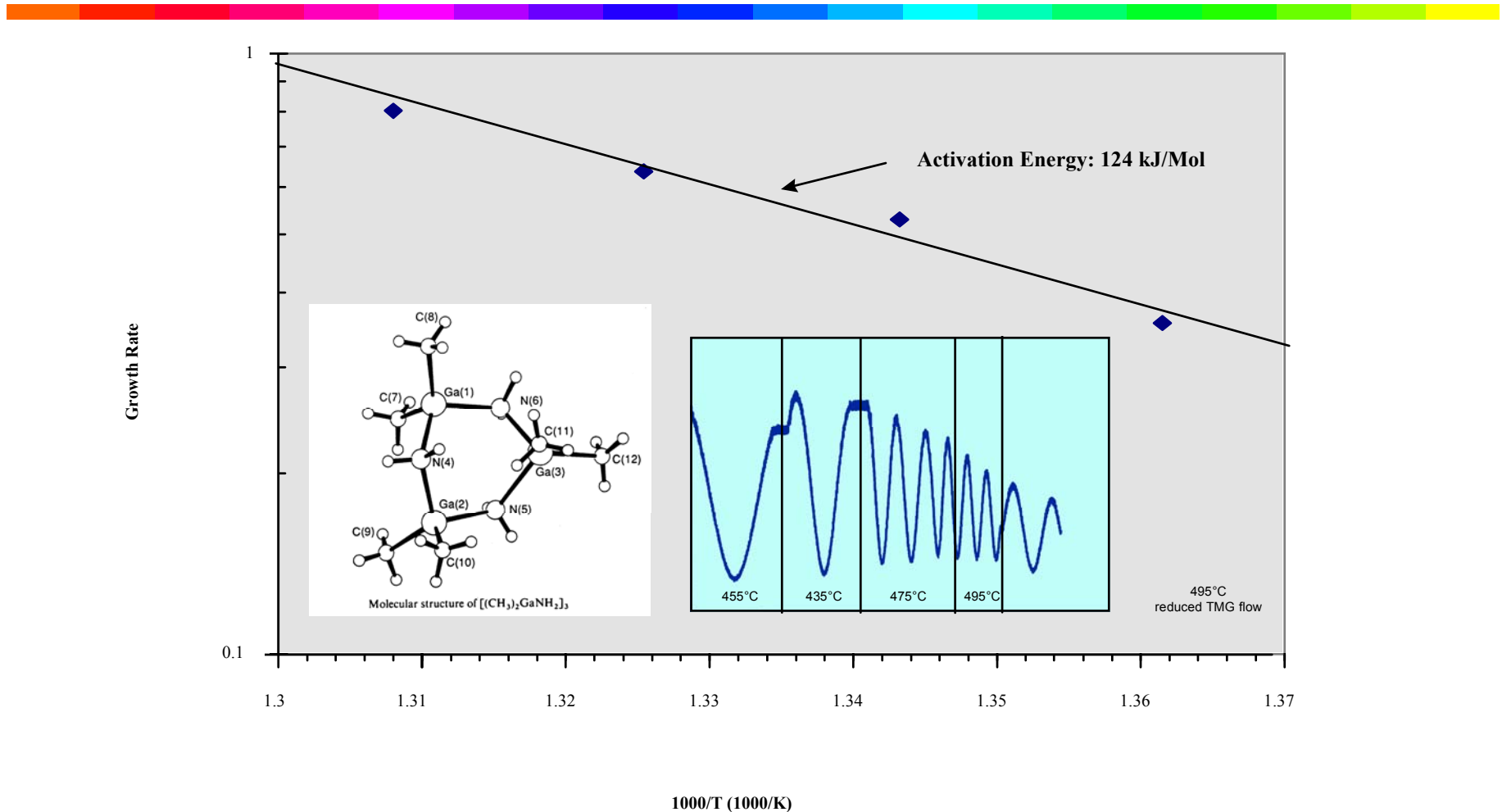


	GaN	Sapphire
Tilt	0.06°	0.02°
Twist	0.13°	0.02°
Lateral	$0.5\text{ }\mu\text{m}$	Infinite

In-situ reflectivity spectrum of GaN



Nucleation layer growth rate vs. temperature

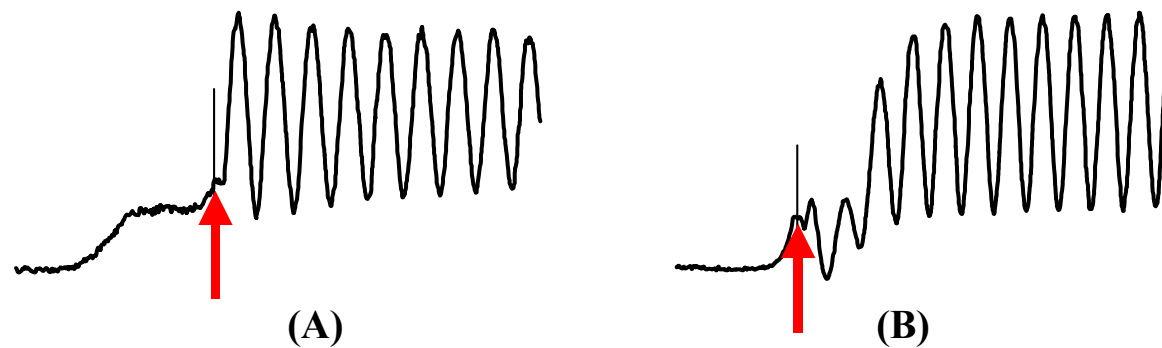


- Evidence for TMGa and NH_3 adduct formation
- Strong temperature dependence

Material Optimization Using *In-Situ* Reflectivity

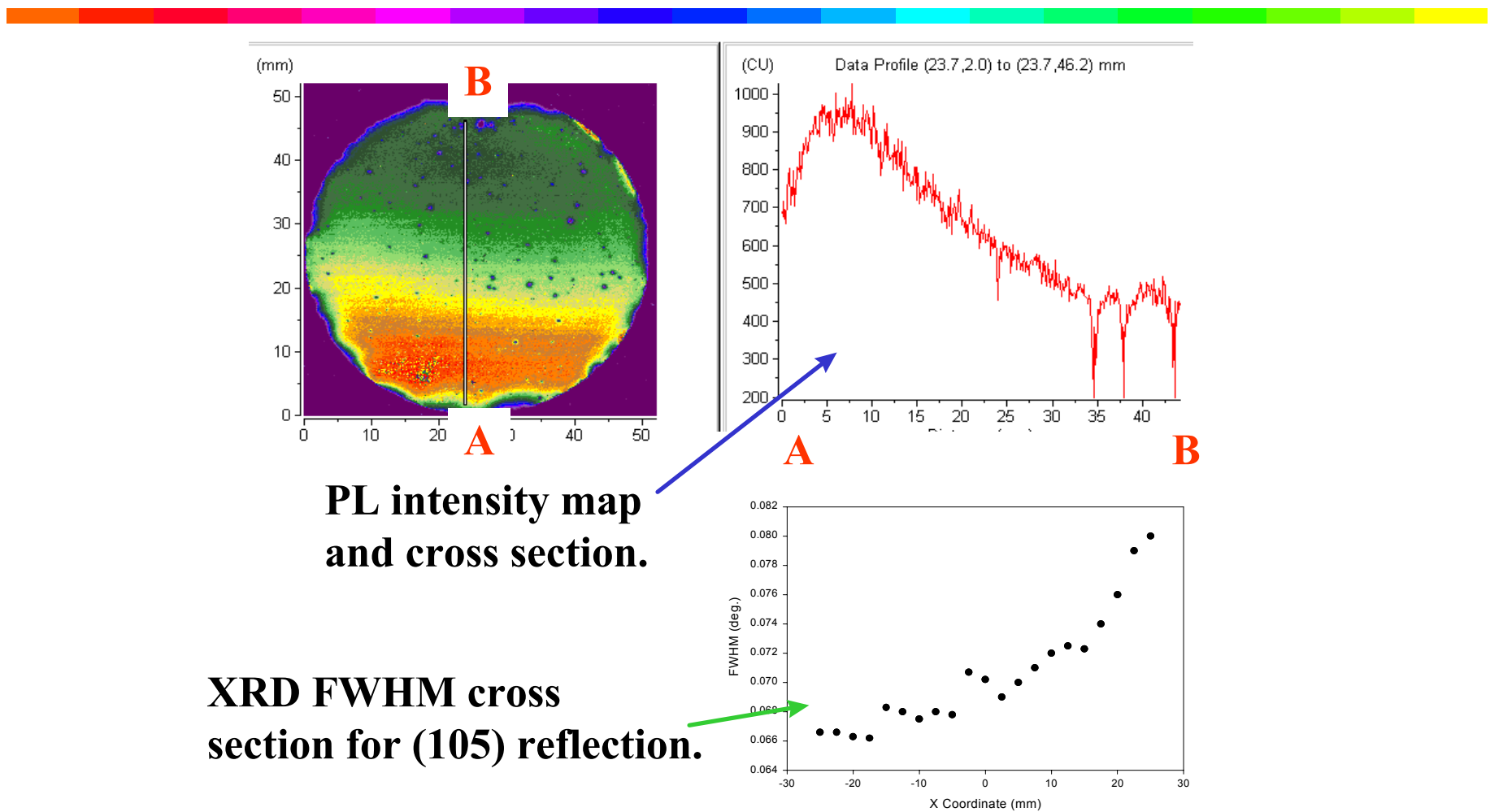


<u>Predominant dislocation</u>	X-Ray Reflection		(B)
	(002)	(102)	
Screw	250 arcsec	400 arcsec	$\sim 10^8 \text{ cm}^{-2}$
Edge	30 arcsec	750 arcsec	$\sim 10^{10} \text{ cm}^{-2}$



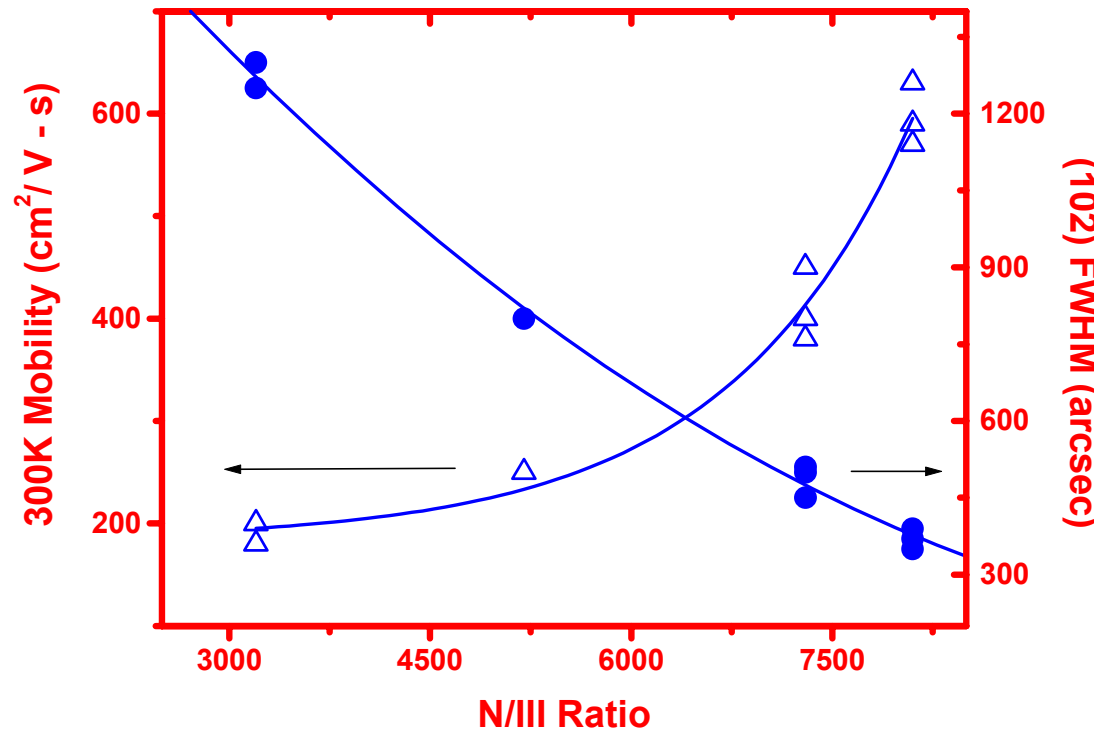
The buffer layer observed by *in-situ* reflectivity shows a strong dependence on defect density. A slow recovery (B) following nucleation results in a lower defect density.

A Comparison of PL Intensity and X-ray FWHM for a GaN Layer



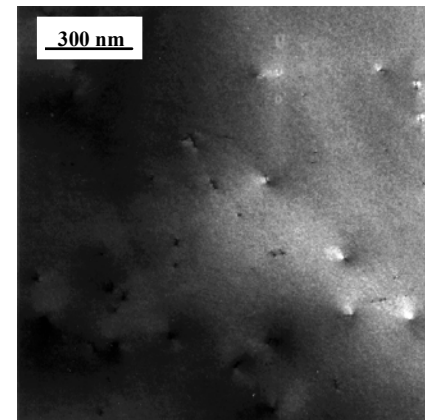
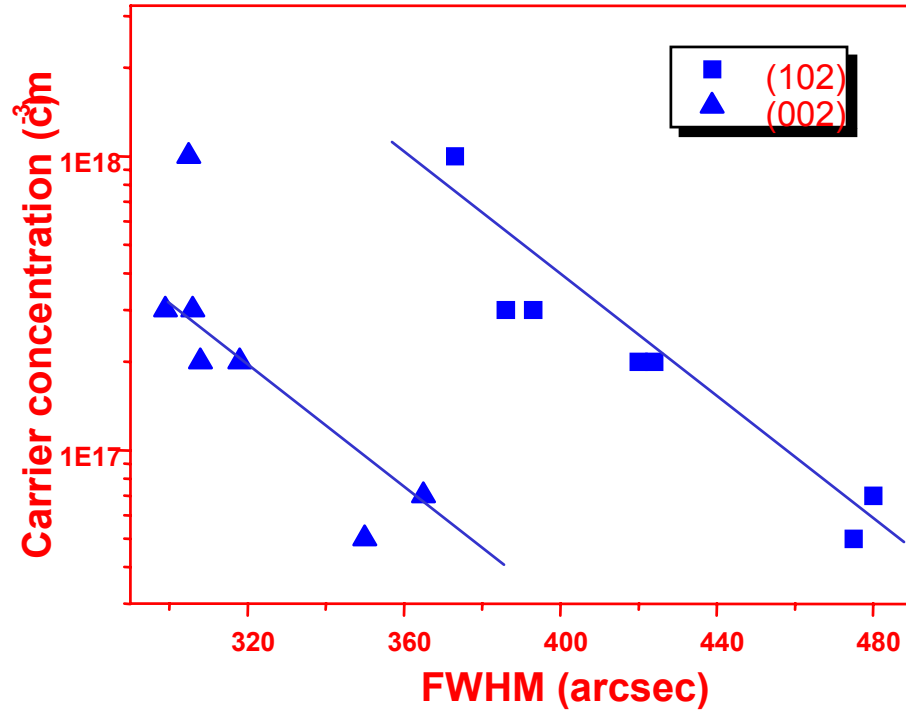
The PL intensity is only sensitive to the XRD reflection that maps the magnitude of twist in the GaN due to edge dislocations.

Electrical Properties of GaN

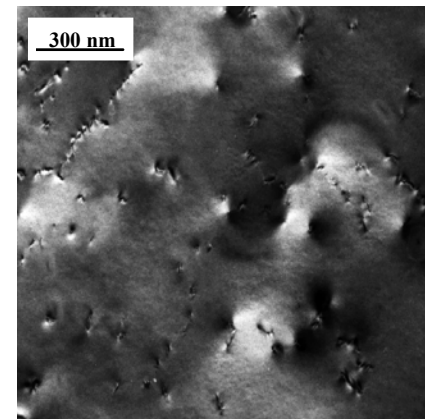


Higher N/III ratio leads to reduced
defects and higher mobility

Growth of p - GaN



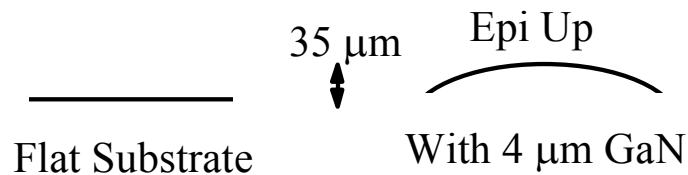
Undoped GaN (Defect density: $1.5 \times 10^9 \text{ cm}^{-2}$)



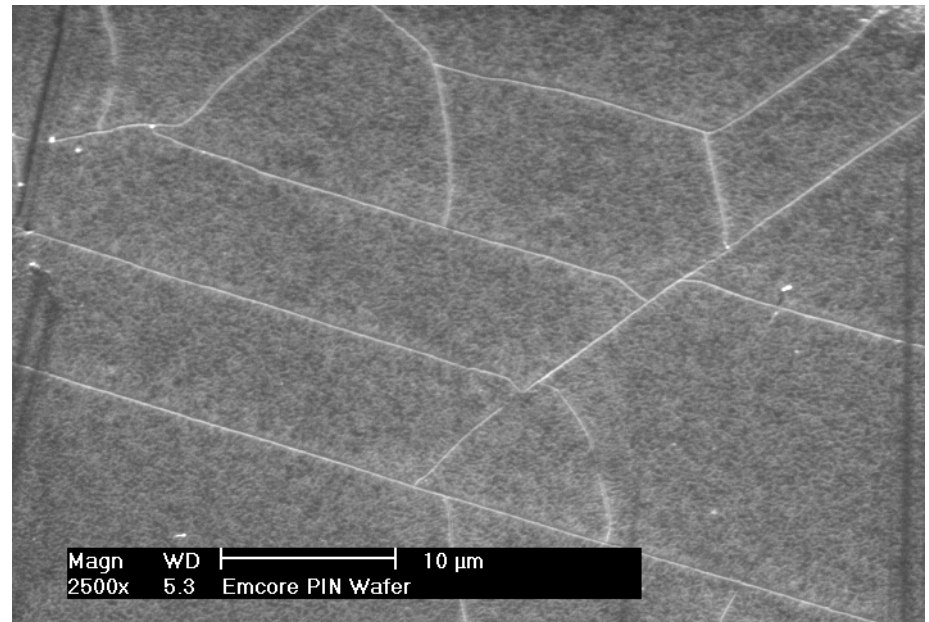
p-GaN (Defect density: $4 \times 10^9 \text{ cm}^{-2}$)

- All films grown with same Cp2Mg flow
- Improved buffer layer growth leads to lower defects and high p-doping level

Epitaxial layer cracking



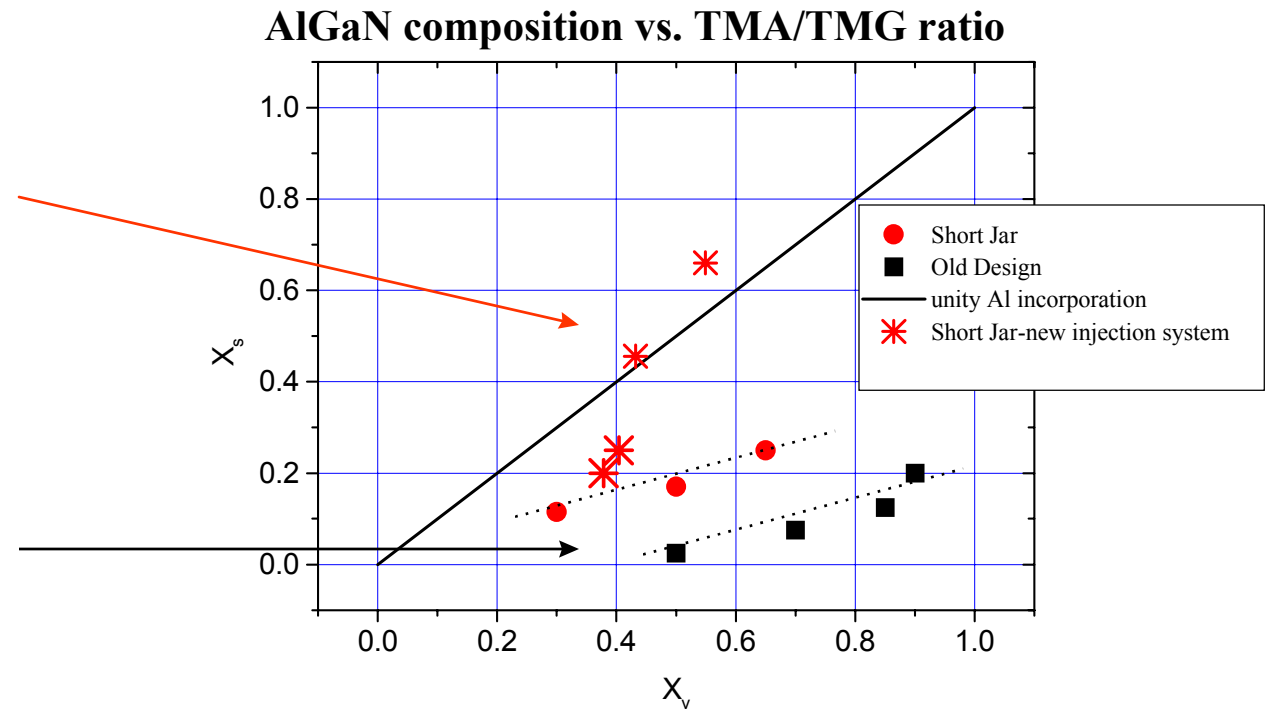
Substrate Thickness	1-side polished Bowing (μm)	2-side polished Bowing (μm)
0.010	31	-
0.013	22	20
0.017	11	-



Sapphire wafer bowing due to the difference in the thermal expansion coefficients for sapphire and GaN (7.3 vs. 5.6 ppm/K, a-plane)

Cracking density depends on layer thickness and doping concentration and is still under investigation

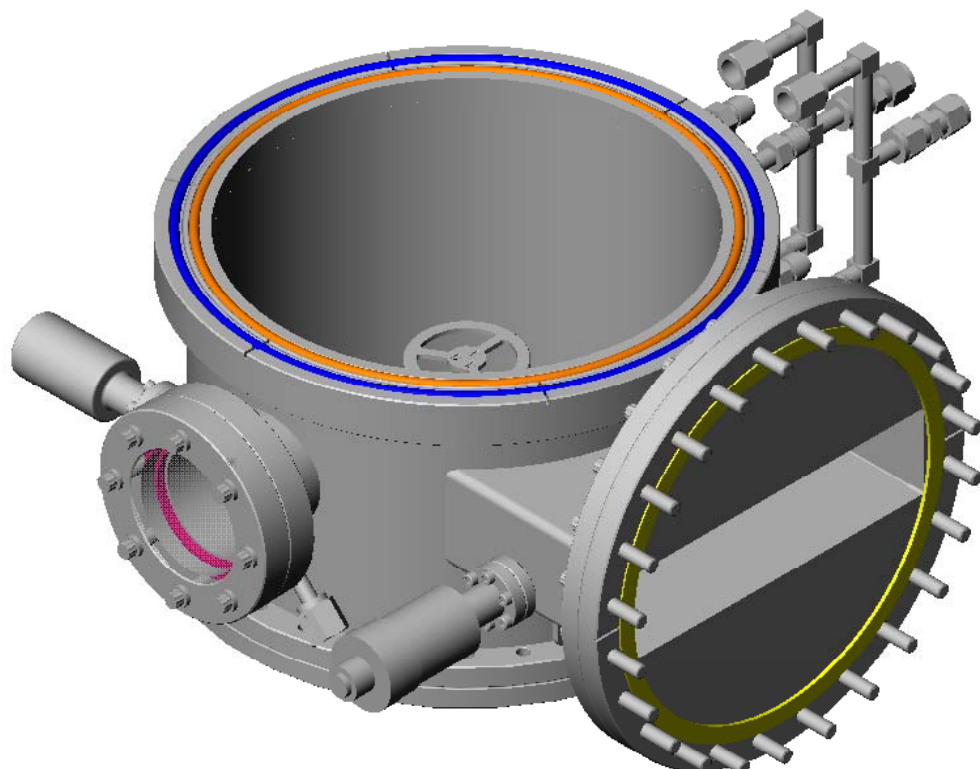
Improving Al Incorporation Efficiency



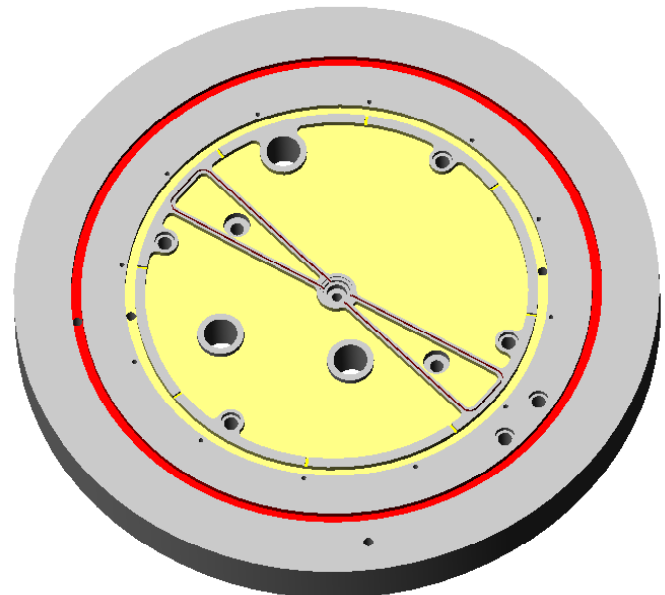
Improvements in the reactor design and growth condition:

- Reduced pre-reactions
- Yielded higher Al incorporation efficiency (approaching unity incorporation)
- Growth rates: 0.3 $\mu\text{m}/\text{h}$ and 0.2 $\mu\text{m}/\text{h}$ for 46% and 66% AlGaN, respectively

GaN D180 Short Jar Geometry



Reactor Chamber



Injection plate

AlGaN pre-reactions and deposition inside reactor



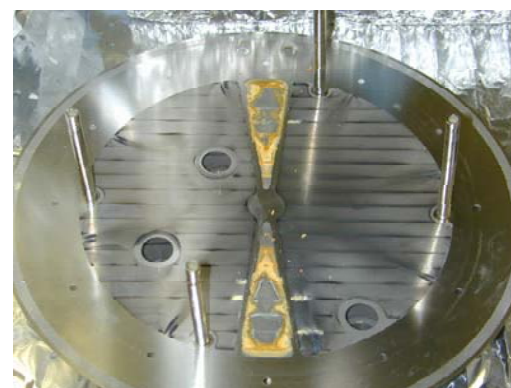
Cracked platter



Inside the reactor



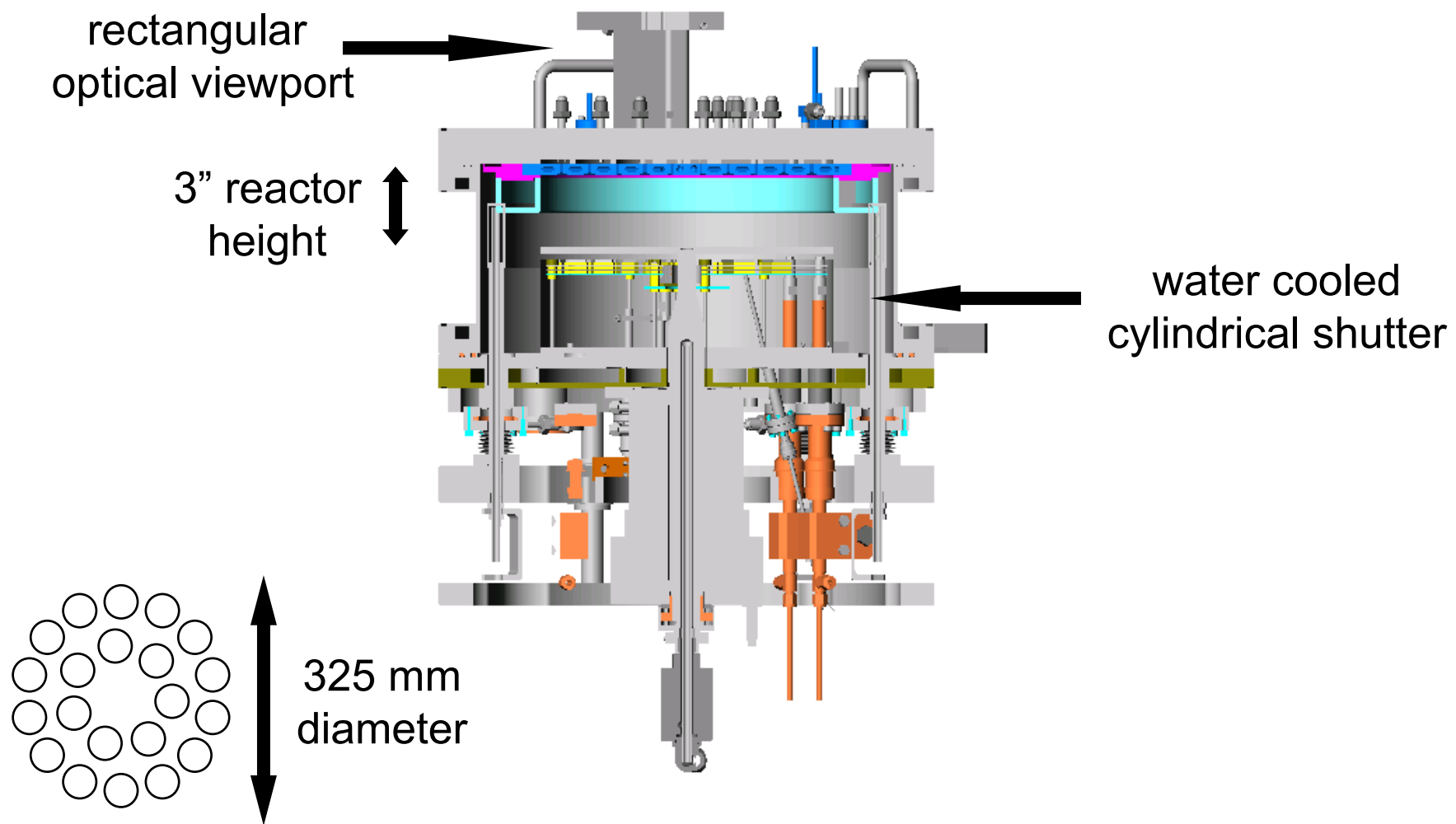
Donut and cold plate



Etch screen and deposition

Developed an in-situ HCl etch

Large Area GaN Reactor Design

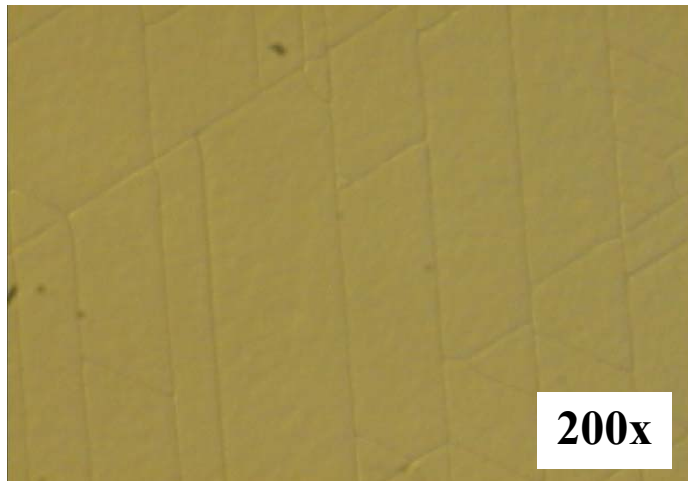


Optical Microscope Image of the AlGaN Surface

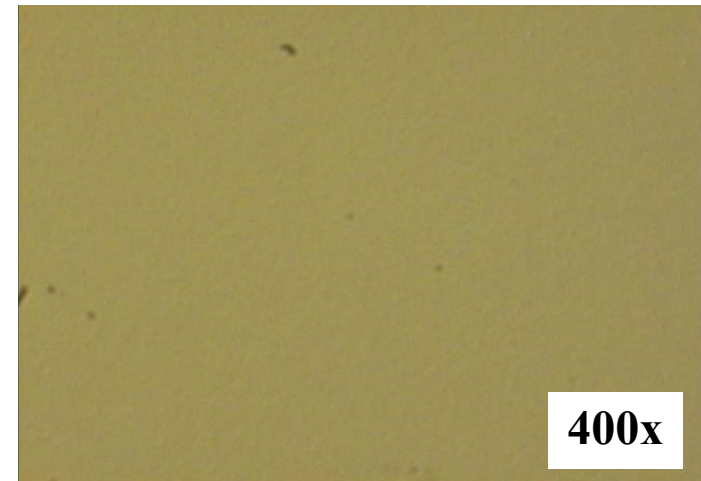


Surface cracking in high Al% concentration AlGaN

Old AlGaN, 60%Al



New AlGaN, 60%Al



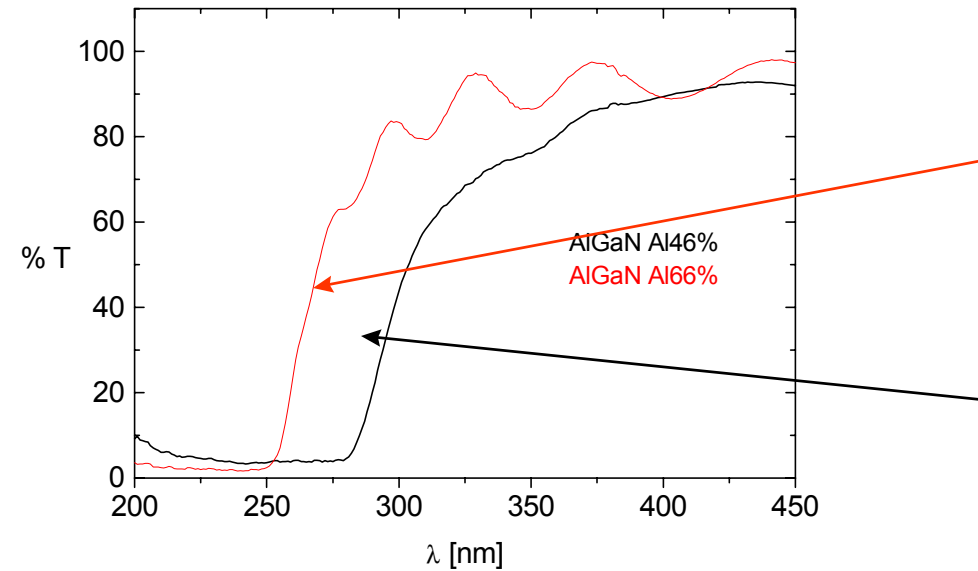
Surface cracking addressed by:

- Optimization of low temperature buffer layer
- Varying the growth cooling/heating ramps
- Optimization of the AlGaN growth rate

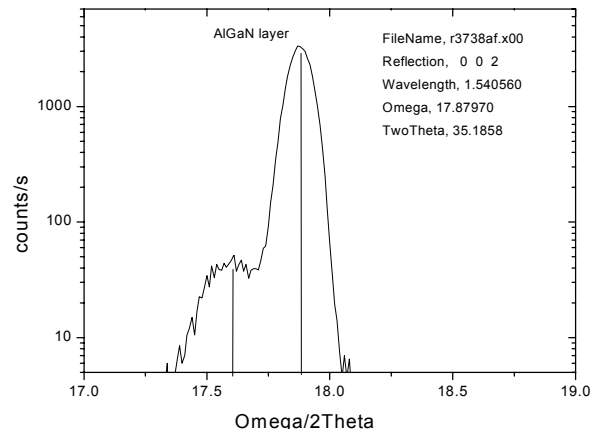
Properties Si of doped AlGaN



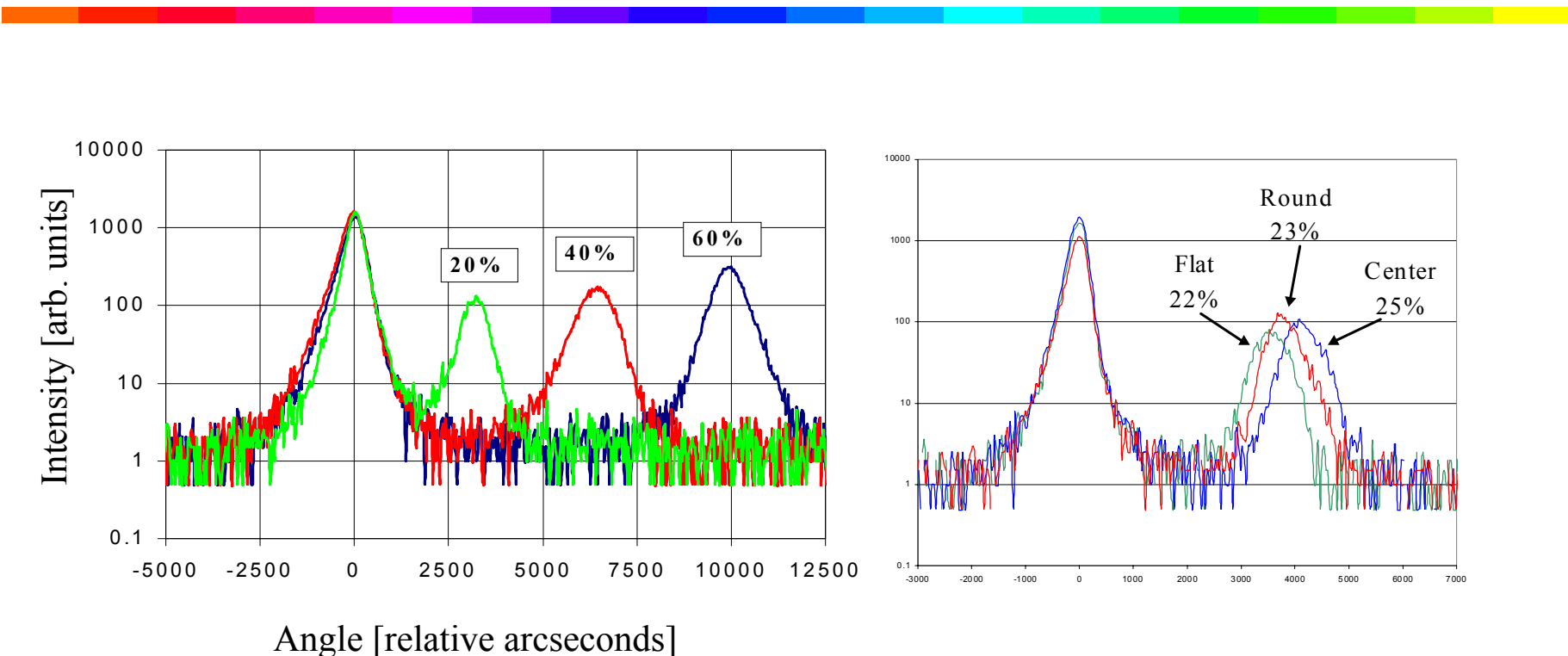
	<u>40%Al</u>	<u>60%Al</u>
Lehighton (Ω / \square)	3.0e3	3.4e4
XRD 002 (arcsec)	370	390
Hall μ ($\chi\mu^2/\zeta\sigma$)	65	5
Hαλλ N ($\chi\mu^{-3}$)	4ε17	3ε17



XRD 002 FWHM = 380 arcsec

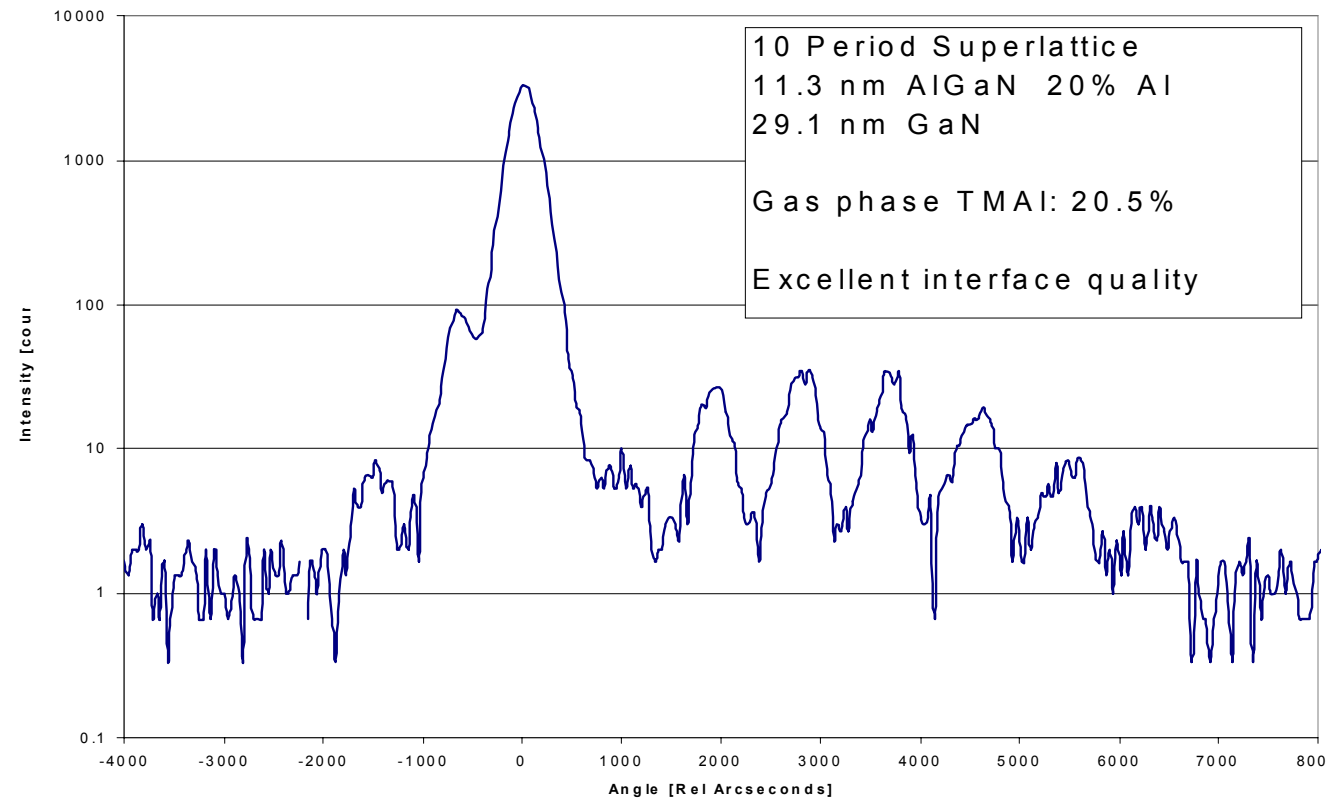


XRD for thick AlGaN films



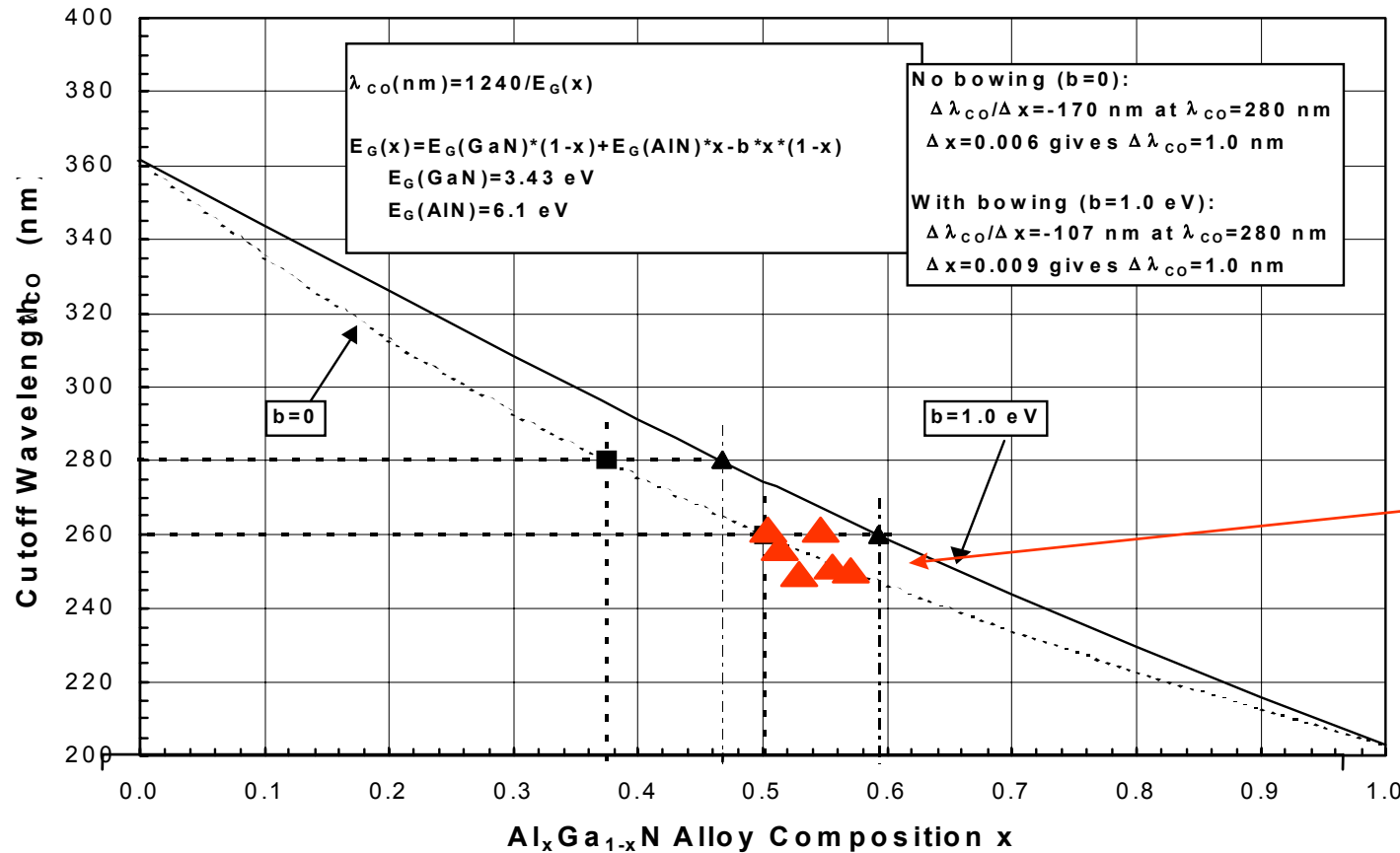
- Good crystal quality over a wide range of Al compositions
- Composition $\pm 1.5\%$, Thickness uniformity $<5\%$

AlGaN/GaN Superlattice



- Superlattice structures gives the most accurate measurement of composition and thickness.
- Sharp fringes indicate good interfaces

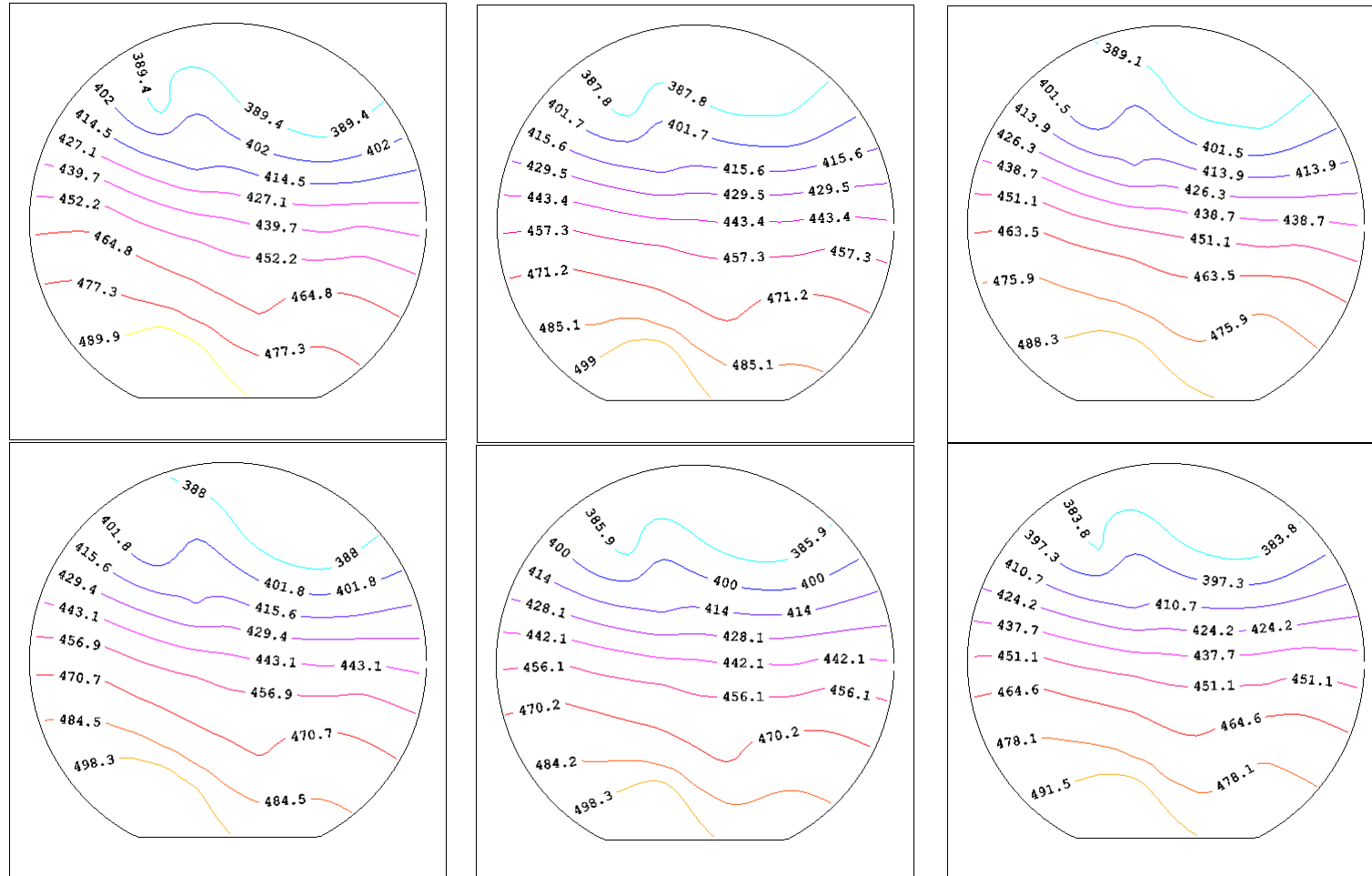
Dependence of cutoff wavelength on AlGaN composition



Recent
data

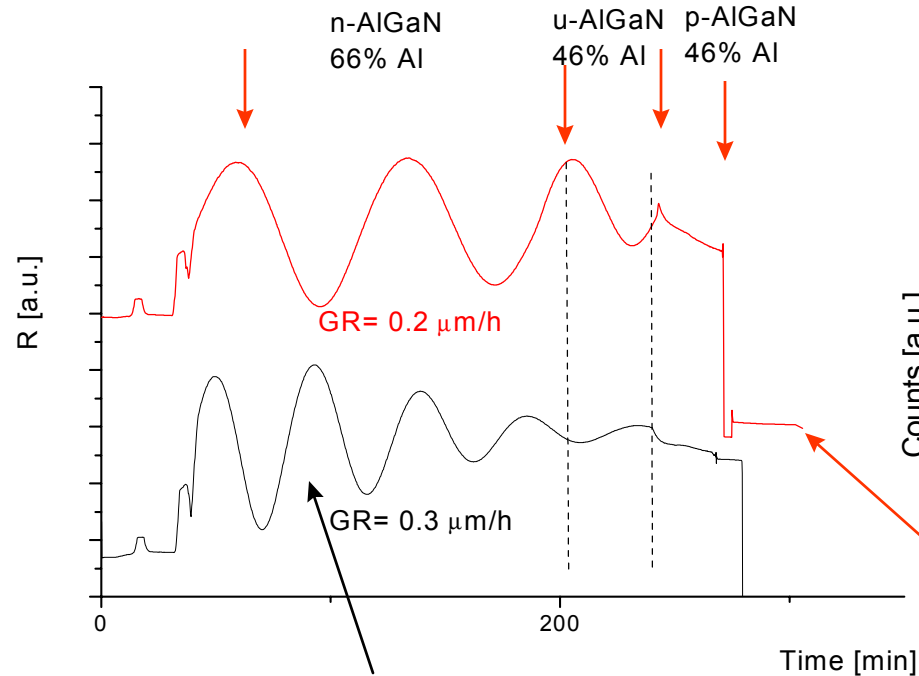
- Initial data appears to have a bowing parameter of 1.0 eV
- Knowledge of Al% composition not well known (estimated XRD 002)
- Effects of compositional fluctuations and ordering not well known

Uniformity of AlGaN/GaN FET Structure



Wafer-to-wafer resistivity variation <0.5%

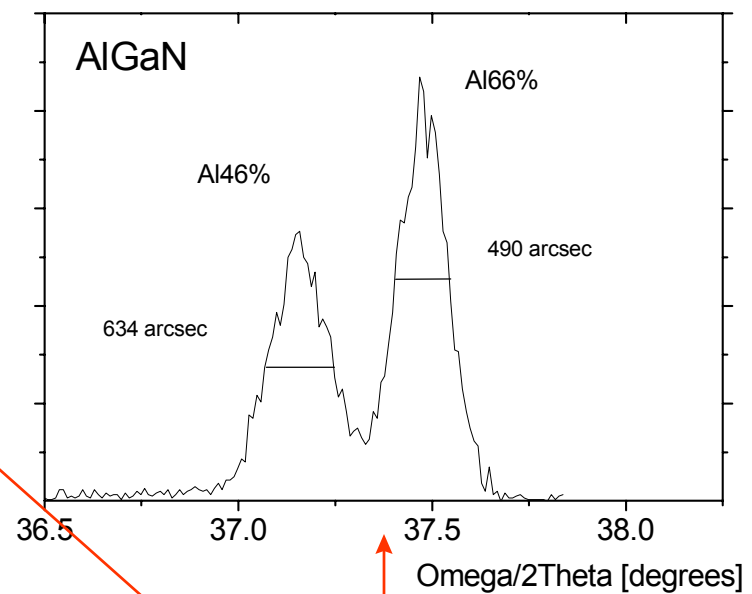
Device optimization using AlGaN reflectivity data



p-i-n AlGaN homostructure

Layer	x	Thickness
p-AlGaN	46 %	0.10 μm
u-AlGaN	46 %	0.15 μm
n-AlGaN	66 %	0.75 μm

XRD 004 was used to resolved peaks and determine Al %

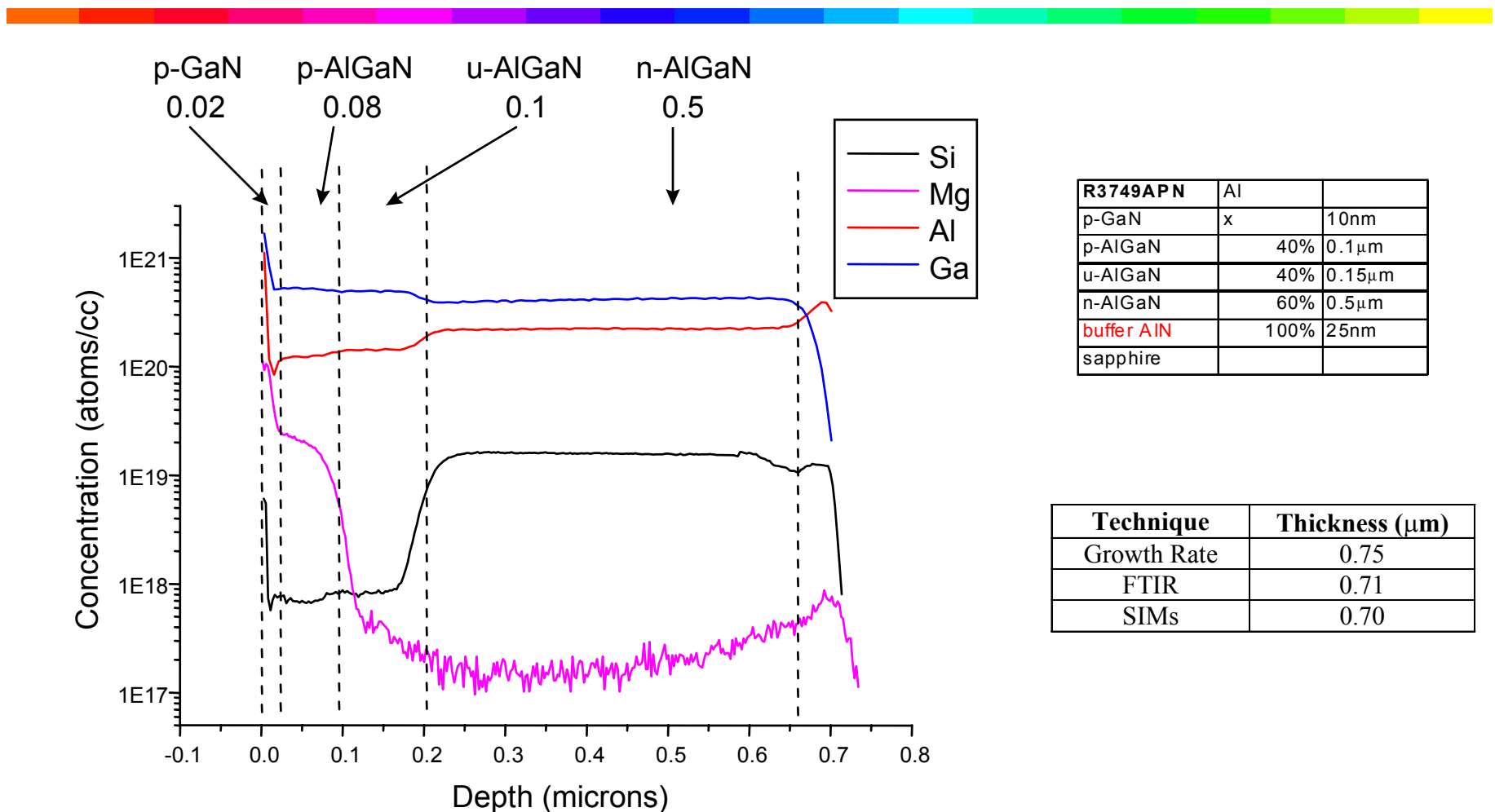


p-i-n AlGaN heterostructure

Layer	x	Thickness
p-AlGaN	46 %	0.10 μm
u-AlGaN	46 %	0.15 μm
n-AlGaN	66 %	0.50 μm

***In-situ* techniques are used for device optimization**

SIMs data for UV detector structure



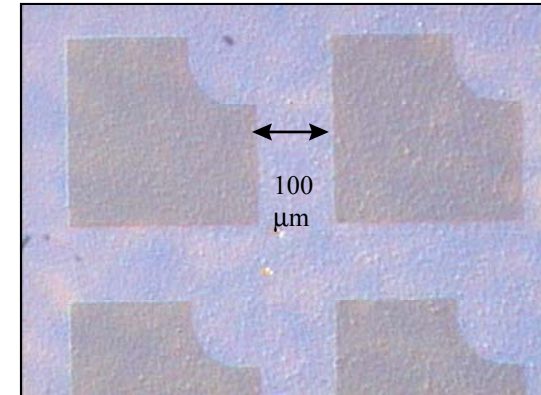
Thickness measured by growth rate, FTIR and SIMs are in agreement

p-AlGaN contact annealing study



Sample # R3842pn

Layer function	x-value	Thickness	Doping
p-AlGaN Cap	0.45	10 nm	Mg-doped-(Max possible)
AlGaN p-type	0.45	0.2 μm	Mg-doped
n-AlGaN	0.45	0.2 μm	~6E17
AlN low-temp. buffer	1.00		
Sapphire substrate			



P-contacts: Au squares 250 x 250 μm
separated by 100 μm

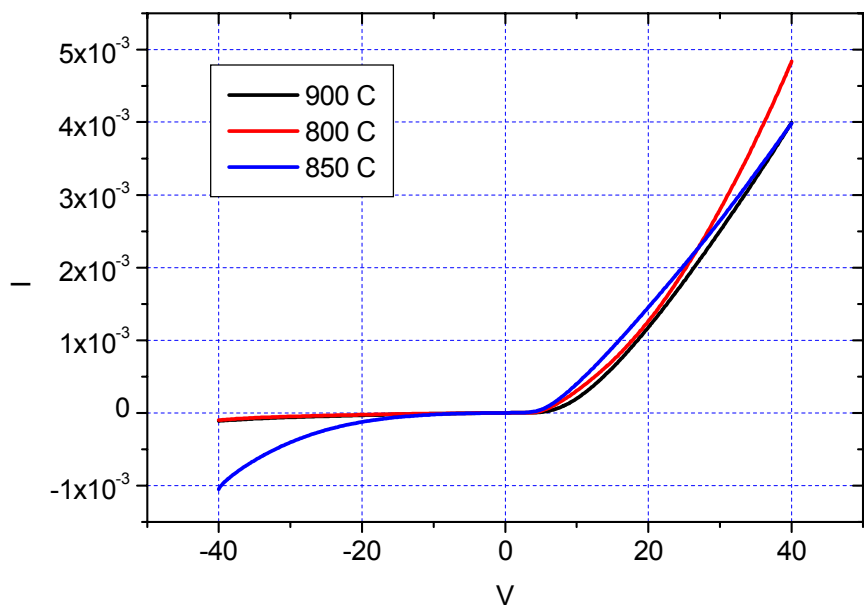
- Investigated activation by RTA at 800 C, 850 C and 900 C for 4 minutes in nitrogen.
- P-contact resistance and the p-n junction forward voltage were measured.

P-contacts were Au squares 250 x 250 μm with 100 μm distance between them
Indium solder was applied as the n-contact

p-AlGaN contact annealing study

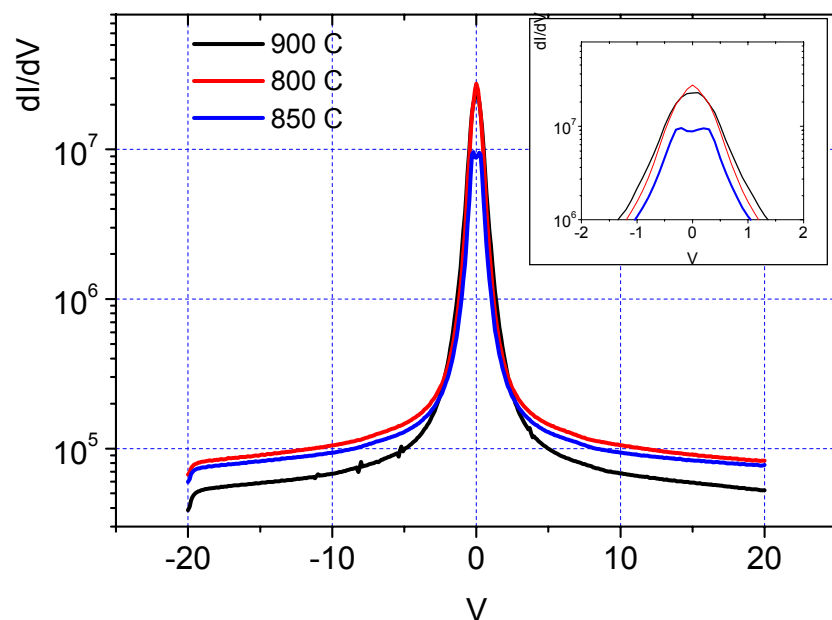


•I vs V for p-n measurements



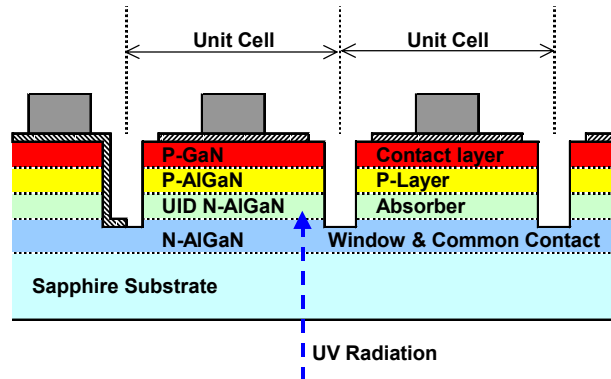
Activation by Rapid Thermal Annealing (RTA) at 850 C for 4 minutes in nitrogen gave the lowest p-contact resistance and the lowest p-n junction forward voltage.

•dI/dV vs V for p-p measurements

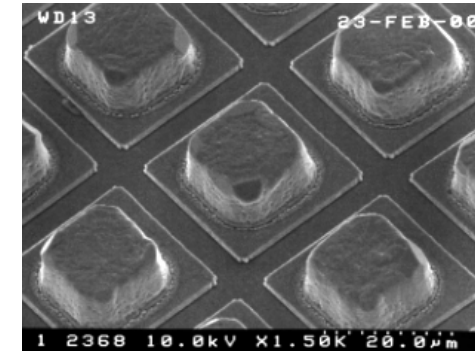


	Annealing temperature (C)	p-p R_0 (ohm)	p-n R_0 (ohm)
R3842apn3	900	2.3E7	2.2E5
R3842apn4	800	2.8E7	5.5E5
R3842apn5	850	9.7E6	1.2E5

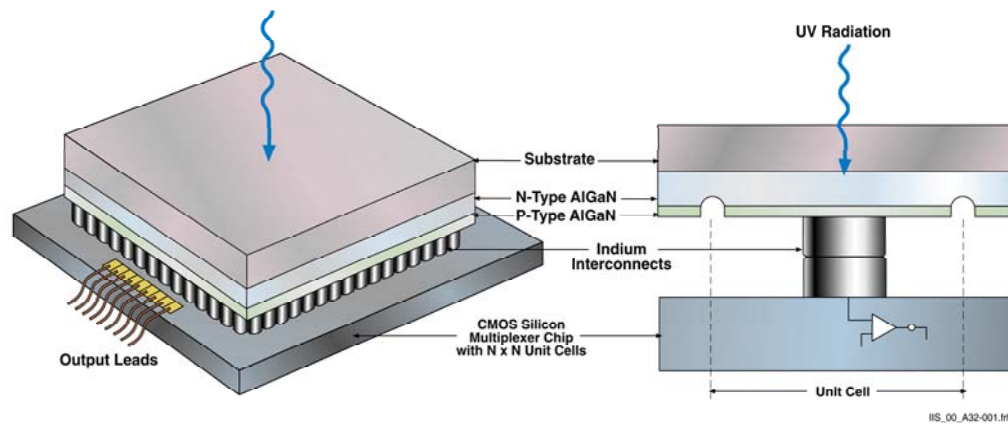
Development of a Hybrid Focal Plane Array



Cross section of the back-illuminated AlGaN p-i-n photodiode array

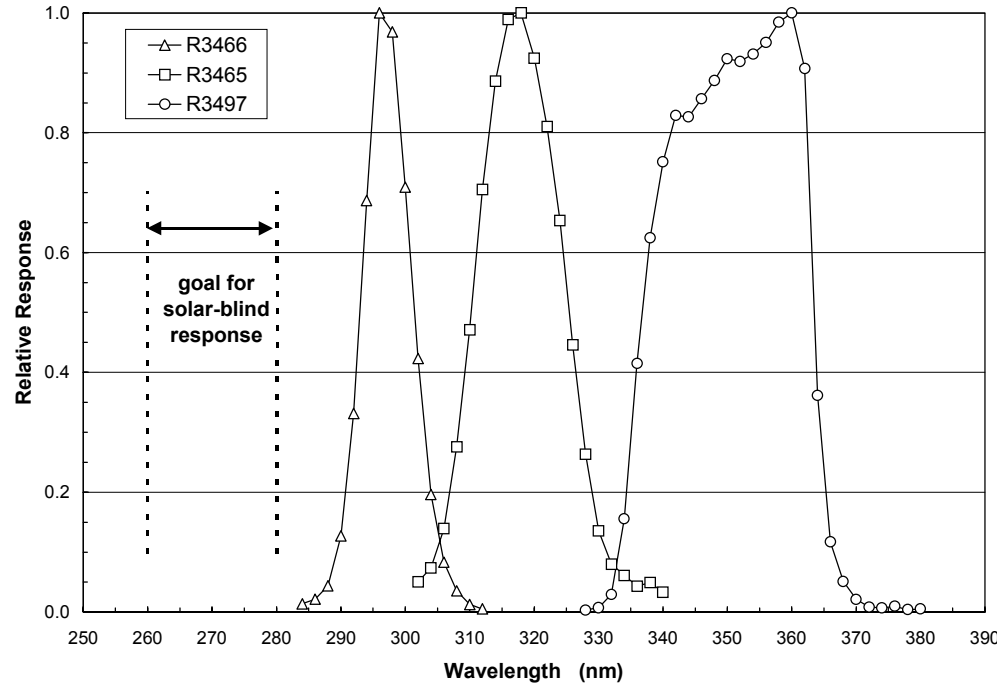


30 \times 30 μm^2 unit cells of an AlGaN array



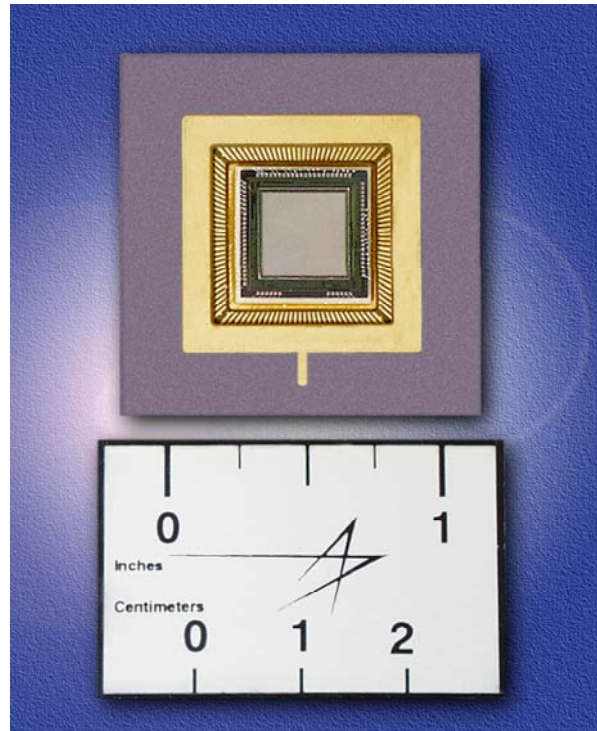
Indium bump interconnects to silicon CMOS ReadOut Integratrd Circuit (ROIC) chip.

Relative spectral response data at zero bias voltage for AlGaN back-illuminated p-i-n photodiodes



Film	Cuton (nm)	Cutoff (nm)	$\Delta\lambda$ (nm)	Window x-value	Absorber x-value	R_0A ($\text{ohm}\cdot\text{cm}^2$)	QE (external)
R3497	337	365	28	0.14	0	$1.5e10$	50% (V=0), 62% (V=-9 V)
R3465	309	326	17	0.30	0.20	$>7e8$	
R3466	293	302	9	0.40	0.34	$>1e9$	7% (V=-1 V)

UV Image Obtained from an AlGaN FPA



A quarter reflecting UV radiation

AlGaN UV detector with 20% Al absorber and 30% Al window

256 x 256 pixel array ~1cm² in area (20 μm² with 30 μm pitch)

Conclusion

**Many technical challenges to produce a UV
emitter at 280 nm based on AlGaN**

Materials and device development issues

- High quality ($x=0.4-0.6$) $\text{Al}_x\text{Ga}_{1-x}\text{N}$
 - Background impurities
 - Ordering
 - DX-like centers
- Doping issues
 - p-doping of AlGaN and contacts
 - n-doping of ($x > 0.4$) $\text{Al}_x\text{Ga}_{1-x}\text{N}$
- Lattice matched growth
 - Cracking